

---

# PIE-NET: Parametric Inference of Point Cloud Edges (Supplementary Material)

---

Anonymous Author(s)

Affiliation

Address

email

## 393 6 Closed curve proposal generation

394 Our closed curve proposal module is inspired by [45]. In particular, we first identify the subset of  
395 points belonging to closed curves via feature *clustering*, and then *fit* a closed curve to each proposed  
396 cluster, while simultaneously estimating the *confidence* of the fit; see Figure 10. Here we use the  
397 edge/corner classification described in Section 3.1 of the main paper. Note our method currently only  
398 handles curves with a *circular* profile, but it can be easily extended to other types of closed curves.

399 **Clustering.** We train an equivariant PointNet++ network to produce a point-wise feature  $F(\cdot)$  for each  
400 of the  $M$  input edge points. Based on such features, we then create a similarity matrix  $S \in \mathbb{R}^{M \times M}$ ,  
401 where  $S_{ij} = \|F(p_i) - F(p_j)\|_2$ . We can then interpret each of the  $M$  rows of  $S$  as a *proposal*, and  
402 consider the set  $C_m = \{j \text{ s.t. } S_{m,j} < \bar{S}\}$  as the edge points of the  $m$ -th proposal.  $\bar{S}$  is a threshold to  
403 filter out the points attaining very different feature scores (i.e., they probably do not belong to the  
404 same curve). Potentially redundant proposals are dealt with in the *selection* phase of our pipeline, as  
405 described in Section 7.

406 **Fitting.** We take each proposal  $C_m$ , and regress the parameters  $\beta$  of the corresponding  
407 curve, as well as its confidence  $\gamma$ . We parameterize each circle proposal via three points  
408  $\beta = \{p_a + \Delta_a, p_b + \Delta_b, p_c + \Delta_c\}$ . We obtain  $\{p_a, p_b, p_c\}$  by furthest point sampling in  $C_m$  initialized  
409 with  $p_a = p_m$ . We then train a PointNet architecture with two fully-connected heads. The first head  
410 regresses the offsets  $\{\Delta_a, \Delta_b, \Delta_c\}$ , while the second head predicts  $\gamma$ .

411 **Losses.** We train our network to predict similarity matrices  $S$  given ground truth  $\hat{S}$ , confidences  
412  $\Gamma = \{\gamma_n\}$  given ground truth  $\hat{\Gamma}$ , and a collection of points sampling the ground truth curve:

$$\mathcal{L}_{\text{closed}} = \mathcal{L}_{\text{sim}}(S, \hat{S}) + \mathcal{L}_{\text{score}}(\Gamma, \hat{\Gamma}) + \mathcal{L}_{\text{para}}(\beta). \quad (5)$$

413 Given that  $\hat{S}_{ij} = 0$  if points  $p_i$  and  $p_j$  belong to the same ground truth curve and  $\hat{S}_{ij} = 1$  otherwise, we  
414 supervise for similarity via:

$$\mathcal{L}_{\text{sim}} = \sum_{ij} S_{ij}, \quad (6)$$

where

$$S_{ij} = \begin{cases} \|F(p_i) - F(p_j)\|_2, & \hat{S}_{ij} = 1 \\ \max\{0, K - \|F(p_i) - F(p_j)\|_2\}, & \hat{S}_{ij} = 0 \end{cases}$$

415 where  $F$  is point-wise feature computed with PointNet++.  $K$  controls the dissimilarity between  
416 elements in different parts, which is set to  $K=100$  in our experiments. For  $\mathcal{L}_{\text{score}}(\cdot)$  we employ  $L_2$   
417 loss, where  $\hat{\Gamma}$  is the segmentation confidence. Positive training examples come from seed points  
418 belonging to ground truth closed curves, and their IoU with ground truth segmentations is larger than  
419 0.5. Negative training examples are those with IoU smaller than 0.5. For parameter regression, we  
420 minimize

$$\mathcal{L}_{\text{para}} = \hat{T}_{\text{circle}} \cdot \mathcal{L}_{\text{circle}}(\beta), \quad (7)$$

421 where  $\hat{T}_{\text{circle}}$  is the ground truth one-hot labels, and  $\mathcal{L}_{\text{circle}}(\cdot)$  is the Chamfer distance between the  
422 curve represented by  $\beta$  and the ground truth. In particular, we first compute the circle according to

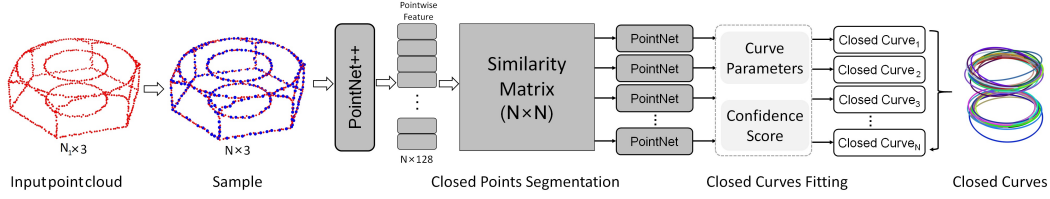


Figure 10: **Closed curve proposal** – We first identify the subset of points belonging to closed curves via feature-based clustering and then fit a closed curve to each cluster. The network outputs both curve parameters and confidence scores.

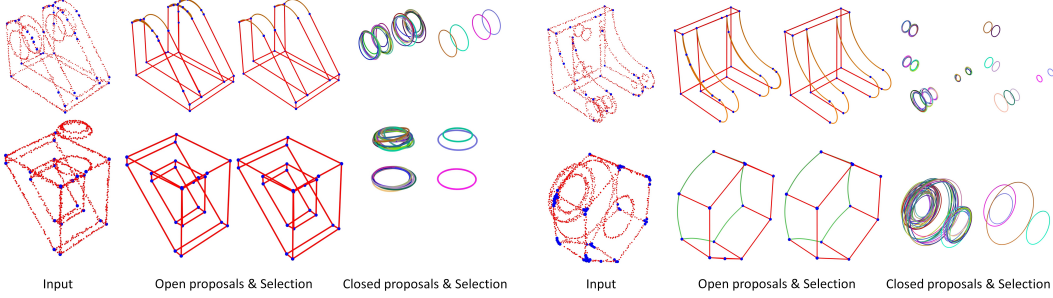


Figure 11: **Proposal selection** – The curves generated by open/closed proposals, and the ones that were accepted by our selection process.

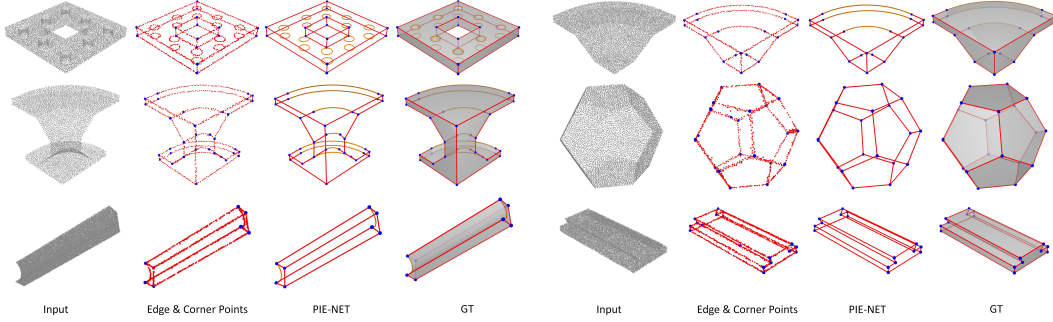


Figure 12: Results on edge and corner detection and parametric curve inference by PIE-NET.

423 the estimated  $\beta$ , and then sample it by points. We then compute the Chamfer distance between the  
 424 estimated circle and its corresponding point-sampled ground-truth.

## 425 7 Curve proposal selection

426 Similar to proposal-based object detection for images [44], the final stage of our algorithm is a  
 427 non-differentiable process for redundant/invalid proposal filtering; see Figure 11. We adopt slightly  
 428 different solutions for *open* and *closed* curves.

429 **Open curve selection.** Given the segmentations, i.e., a set of points associated with a curve (see  
 430 Figure 5 in the main paper) corresponding with two proposals, we first measure overlap via  $O(A, B) =$   
 431  $\max\{I(A, B)/A, I(A, B)/B\}$ , where  $I(A, B)$  is the cardinality of the intersection between the sets.  
 432 We then merge the two candidates, if  $O(A, B) > \tau_o$  and retain the curve with larger cardinality, where  
 433 we use  $\tau_o = 0.8$  as determined by hyper-parameter tuning.

434 **Closed curve selection.** The similarity matrix produces a closed-curve proposal for *each* of its  $N$   
 435 rows. Even after discarding proposals with confidence score  $\gamma_n < \tau_\gamma$ , many are *non-closed* curves, or  
 436 represent the *same* closed curve; see Figure 11. We perform agglomerative clustering for proposals  
 437 when  $\text{IoU}(A, B) > \tau_{\text{IoU}}$ , and retain the proposal in the cluster with the highest confidence. We use

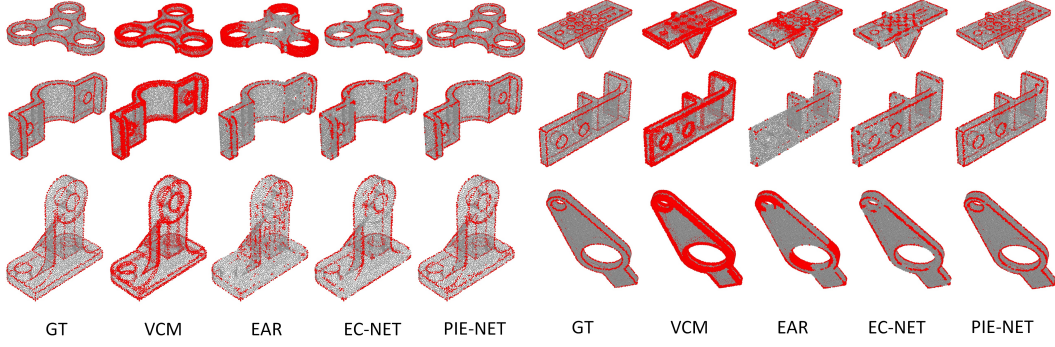


Figure 13: **Comparisons to state-of-the-art methods** – Qualitative comparisons against edge detection techniques – VCM [50], EAR [51], and EC-Net [10].

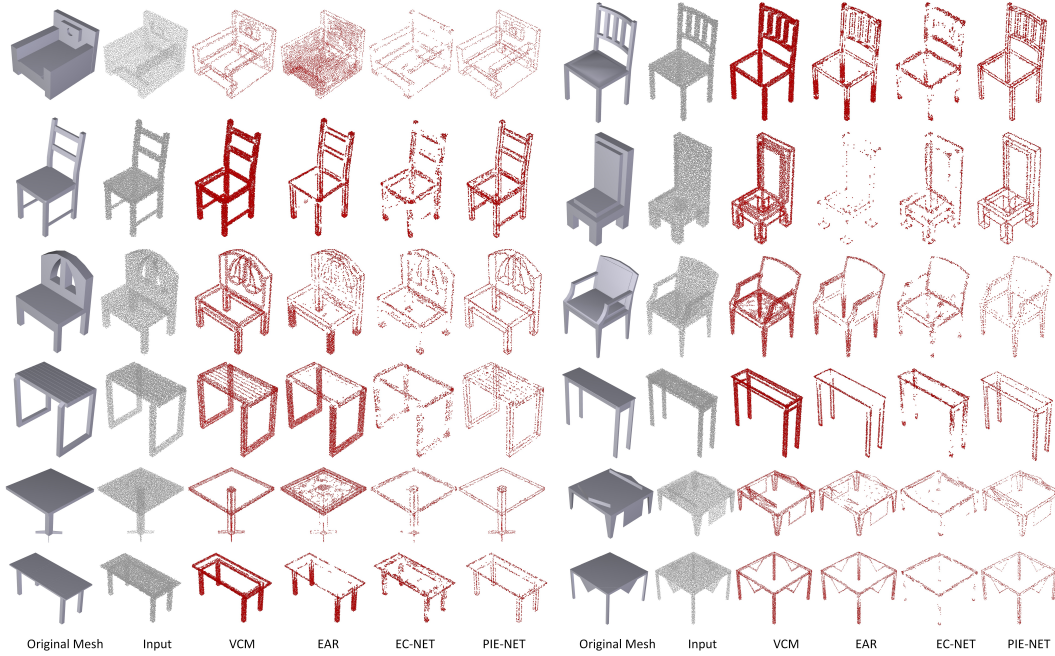


Figure 14: **Generalization to novel object categories** – While PIE-NET is trained on CAD models of mechanical assemblies from the ABC dataset [46], our edge detector is immediately applicable to 3D point clouds of general 3D objects and consistently outperforms VCM, EAR, and EC-Net.

438  $\tau_\gamma=0.6$  and  $\tau_{100}=0.6$  for all our experiments. Finally, for each closed segment, we select the best  
 439 matching closed curve. Specifically, we use the Chamfer Distance to measure the matching score.

## 440 8 Backbone architectures

### 441 8.1 Classification

442 We use PointNet++ [47] as the feature backbone network. Following the same notations in Point-  
 443 Net++,  $SA(K, r, n, [l_1, l_2, \dots, l_d])$  is a set abstract layer with  $K$  local regions of balls with radius  $r$ .  $n$   
 444 points are sampled for each local region. The SA layer uses  $d$  1\*1 conv layers with output channels  
 445  $l_1, l_2, \dots, l_d$  respectively.  $FP(l_1, l_2, \dots, l_d)$  is a feature propagation (FP) layer with  $d$  1\*1 conv layers,  
 446 whose output channels are  $l_1, l_2, \dots, l_d$ . In our task, we use four set abstract (SA) layers and four  
 447 feature propagation (FP) layers. The parameters of set abstract (SA) and feature propagation (FP)  
 448 layers are as follows:  $SA(4096, 0.05, 32, [32, 32, 64])$ ,  $SA(2048, 0.1, 32, [64, 64, 128])$ ,  $SA(1024,$   
 449  $0.2, 32, [18, 128, 256])$ ,  $SA(512, 0.4, 32, [256, 256, 512])$ ,  $FP(256, 256)$ ,  $FP(256, 256)$ ,  $FP(256, 128)$ ,

450 FP(128,128,128). Following PointNet++, we also added four separate fully-connected layers in order  
 451 to predict the following tasks: edge point classification  $\hat{T}_e$ , point-to-curve distance vector regression  
 452  $\hat{D}_e$ , corner point classification  $\hat{T}_c$  and corner point residual vector regression  $\hat{D}_c$ .

## 453 8.2 Open curve proposal

454 For each corner pair, we use a PointNet++ as the backbone with two multi-layer perceptrons (MLP)  
 455 layers.  $\text{MLP}([l_1, \dots, l_n])$  indicates several MLPs with output channels  $l_1, \dots, l_n$ . The parameters  
 456 of these two MLPs are set to [128,256, 512], [256, 256]. Following PointNet, we added three  
 457 separate fully-connected layers in order to predict the following tasks: curve segmentation, curve  
 458 type classification, and curve parameters estimation.

## 459 8.3 Clustering

460 We use a PointNet++ as the clustering backbone. In our task, we use four set abstract (SA) layers and  
 461 four feature propagation (FP) layers. The parameters of set abstract (SA) and feature propagation  
 462 (FP) layers are as follows: SA(512, 0.1, 32, [32,32,64]), SA(256, 0.2, 32, [64,64,128]), SA(128,  
 463 0.4, 32, [18,128,256]), SA(64, 0.8, 32, [256,256,512]), FP(256,256), FP(256,256), FP(256,128),  
 464 FP(128,128,128). Following PointNet, we added one MLP layer in order to predict similarity matrix.

## 465 8.4 Closed curve fitting

466 In this task, we use a PointNet as the backbone with two MLP layers. The parameters of the two MLPs  
 467 are set to [128,256, 512], [256, 256]. Following PointNet, we added two separate fully-connected  
 468 layers to predict the curve parameters and the confidence scores.